



SYNTHESIS, CHARACTERIZATION, THEORETICAL STUDIES AND BIOLOGICAL ACTIVITIES OF NARINGIN METAL COMPLEXES

REHAB ABDULMAHDI AL-HASSANI*, OLFATA NIFE and
AYAD T. MAHMOOD^a

Department of Chemistry, College of Science, Al-Mustansiriyah University, BAGHDAD, IRAQ

^aDepartment of Chemistry Polymer research, College of Science, Al-Mustansiriyah University, BAGHDAD, IRAQ

(Received : 10.09.2015; Accepted : 20.09.2015)

ABSTRACT

The new metal complexes of Cr(III), Mn(II), Fe(III), Co(II), Ni(II) and Zn(II) with naringin (L) were synthesized and characterized by elemental and thermal analyses as well as FT-IR and UV-Vis spectra. The magnetic properties and electrical conductivities of metal complexes were also determined. The nature of the complexes formed in ethanol was studied following the mole ratio method. The work also include a theoretical treatment of the formed complexes in the gas phase. This was done using the (hyperchem-8) program for the molecular mechanics and semi-empirical calculations. The heat of formation (ΔH_f°), binding energy (ΔE_b) and total energy (ΔE_T) for ligand and its complexes were calculated by (PM3) method at 298 K. The electrostatic potential of the free ligand (L) was calculated to investigate the reactive sites of the molecules. PM3 was used to evaluate the bond length, vibrational and electronic spectra for the ligand (L) and their metal complexes and compared with the experimental values. The theoretical results agreed with those found experimentally. The antibacterial activity for the (L) and its metal complexes were studied against two types of pathogenic bacteriamicro-organisms *Escherichia coli* and *Staphylococcus aureus*. Furthermore, the antifungal activity against two micro-organisms *Candida albicans* and *Aspergillus flavus* were studied for (L) ligand and its metal complexes.

Key words: Flavonoid, Naringin, Metal complexes, Theoretical study, Antimicrobial.

INTRODUCTION

Plant sources are abundant in the common polyphenolic compounds known as flavonoids that are known to possess various types of pharmacological effects including antioxidant, anti-microbial, anti-inflammatory, anti-allergic and anti-cancer activity¹⁻⁵. The importance of the antioxidant activity of these compounds lies in their ability to scavenge free radicals⁶ that are responsible for DNA damage. Naringin, (Fig. 1) a major bioflavonoid in grapefruit has been shown to reduce radiation-induced damage to DNA⁷. It also acts as the inhibitor of VEGF release, which causes angiogenesis⁸ and has been proven to be effective against ethanol injury in rats⁹. The chemopreventive role of naringin against protoxicants, its action as anti-atherogenic agents in rabbits and its ability to significantly reduce the level of total cholesterol have also been established¹⁰⁻¹². The oral bioavailability of quinine in rats has been shown to increase after pretreatment with naringin¹³. Naringin and hesperidin are the main citrus flavonoids with physiological properties present in grapefruit and orange juice^{10,12}. These flavonoids have been detected in human plasma after orange and grapefruit diets³. There are numerous reports of HPLC analysis of the composition of commercial juices,

concentrates, fresh oranges, and grapefruit³⁻⁵. This paper describes the synthesis of Cr(III), Mn(II), Fe(III), Co(II), Ni(II) and Zn(II) transition metals complexes bearing a naringin ligand, and its characterization by (FT-IR and Uv-Vis) Spectroscopy, elemental analysis and flame atomic absorption techniques as well as magnetic susceptibility and conductivity measurements. The antimicrobial activity for naringin (**L**) and its metal complexes were studied and compared with the corresponding free flavonoid, naringin. The theoretical studies of the naringin (**L**) and their metal complexes were also made and compared with experimental results.

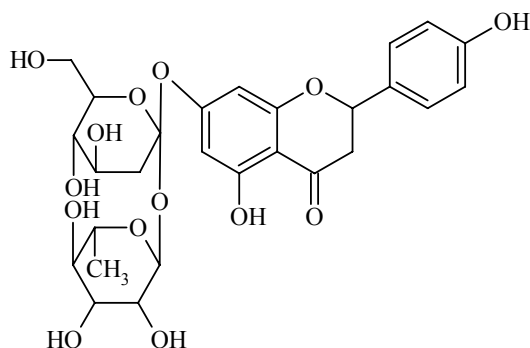


Fig. 1: Structure of Naringin

EXPERIMENTAL

Instrumentation

Melting points were recorded on a Gallenkamp MF B600 melting point apparatus. Elemental analyses (C.H.N.) were obtained using EA-034.mth. For metal complexes of naringin (**L**), metal contents of complexes were estimated spectrophotometrically using Flame atomic absorption Shimadzu-670 AA Spectrophotometer. Infrared spectra were recorded using FT-IR-8300 Shimadzu in the range of 4000-350 cm^{-1} , samples were measured as CsI disc. Magnetic susceptibilities of samples in the solid state were measured by using a Bruker BM6 magnetic balance. The molar conductivity was measured by using electrolytic conductivity measuring set Model MC-1-Mark V by using platinum electrode (EDC 304) with cell constant (1 cm^{-1}), concentration (10^{-3} M) in dimethylformamide as a solvent at room temperature. Electronic spectra were obtained using UV-1650PC-Shimadzu spectrophotometer at room temperature; the measurement were recorded using a concentration of (10^{-3} M) of the metal complexes in dichloromethane as a solvent.

Materials and methods

All chemical were of highest purity and were used as received.

Preparation of metal complexes (1-6) of (**L**)

An ethanolic solution of each of the following metal ions salts (0.69 mmole) ($\text{CrCl}_3 \cdot 6\text{H}_2\text{O}$, $\text{FeCl}_3 \cdot 9\text{H}_2\text{O}$, $\text{MnCl}_2 \cdot 5\text{H}_2\text{O}$, $\text{CoCl}_2 \cdot 6\text{H}_2\text{O}$, $\text{NiCl}_2 \cdot 6\text{H}_2\text{O}$ and $\text{ZnCl}_2 \cdot \text{H}_2\text{O}$) was added to an ethanolic solution (0.69 mmole) of (**L**) except in the case of [Mn(II), Cr(III) and Fe(III)] (1.38 mmol) of (**L**), with stirring. The resultant pH 6.5 [for Cr(III) and Fe(III)], pH 6.2 [for (Mn(II), Co(II) and Ni(II))] and pH 5.8 [for Zn(II)] were maintained by adding sodium acetate. The reaction mixture was heated under reflux for 2-3 hrs. During this time, a precipitate was formed. The product was filtered off, washed with hot ethanol, followed by cold water and then dried under vacuum. All complexes were identified by elemental analysis (C.H.N), flame atomic absorption, FT-IR and Uv-Vis spectrophotometers, magnetic and conductivity measurements.

Study of complexes formation in the solution

The (1-5) complexes of the (L) ligand with the selected metal ions [Cr(III), Fe(III), Mn(II), Co(II) and Ni(II)], were studied in solution using ethanol as a solvent, in order to determine [M:L] ratio in the prepared complexes, following molar ratio method¹⁴. A series of solutions were prepared having a constant concentration (10^{-3} M) of the hydrated metal chlorides and the (L) ligand. The [M:(L)] ratio was determined from the relationship between the absorbance of the absorbed and the mole ratio of [M:(L)].

Programs used in theoretical calculation

Materials and methods

Hyperchem is a sophisticated molecular modeler, editor and powerful computational package, that is known for its' quality, flexibility and ease of use^{15,16}. It can plot orbital wave functions resulting from semi-empirical quantum mechanical calculations, as well as the electrostatic potential, the total charge density or the total spin density can also be determined during semi-empirical calculation. This information is useful in determining reactivity and correlating calculated results with experimental data.

Computational methods

Semi-empirical quantum mechanical, Molecular mechanics and Mopac 2000.

Types of calculations

The types of prediction possible of molecules are^{17,18}:

- (a) Geometry optimization calculations employ energy minimization algorithms to locate stable structures.
- (b) Bond distances
- (c) Molecular dynamics, which provide the thermodynamic calculations and dynamic behavior of molecules
- (d) Plot the electrostatic potential field (HOMO and LUMO).
- (e) Vibrational spectrum (I.R and Raman spectra).

Study of biological activities for ligand (L) and its metal complexes (1-6)

The biological activities of the ligand (L) and its respective complexes (1-6) were studied against selected types of bacteria, which include *Escherichia coli* and *Staphylococcus aureus* cultivated in nutrient agar medium, DMSO was used as a solvent and as a control, the concentration of the compounds in this solvent were 10^{-3} M.

The new metal complexes (1-6) were tested for their *in vitro* growth inhibitory activity against further pathogenic fungi, i.e., *Candida albicans* and *Aspergillus flavus* on potato dextrose agar medium and incubated at 30°C for 72 hrs. DMSO was used as a solvent and as a control for both techniques. The concentrations of the compounds in this solvent were 10^{-3} M. The inhibition of fungal growth expressed in percentage terms, were determined on the growth in test plates compared to the respective control plates, as given by the Vincent equation¹⁹. Furthermore, the antifungal activity against two micro-organism was calculated by the equation (1).

$$\text{Inhibition \%} = 100 (C - T) / C \quad \dots(1)$$

Where, C = Diameter of fungal growth on the control plate, and T = Diameter of fungal growth on the test plate

RESULTS AND DISCUSSION

Study of complexes in solid state

Elemental analyses

The physical and analytical data of the ligand (**L**) and its metal complexes (**1-6**) are given in Table 1. The results obtained from elemental analysis are in satisfactory agreement with the calculated values. The suggested molecular formula was also supported by spectral measurement as well as magnetic moments. The new complexes (**1-6**) were colored crystalline solids and soluble in CH₂Cl₂, CHCl₃, DMF and DMSO. They were thermally stable and unaffected by atmospheric oxygen and moisture.

Table 1: Physical data for complexes (1-6)

Comp. No.	Color	Melting point	Molar ratio (in ethanol)	Yield (%)	Elemental analysis found calc.			Suggested formula
					C (%)	H (%)	M (%)	
1	Dark green	225	1:2	88	50.78	5.11	4.13	[Cr(C ₂₇ H ₃₀ O ₁₄) ₂ (H ₂ O) ₂] Cl
					50.64	5.00	4.06	
2	Yellowish brown	232	1:2	79	52.02	5.18	4.50	[Mn(C ₂₇ H ₃₀ O ₁₄) ₂ (H ₂ O) ₂]
					51.97	5.13	4.41	
3	Dark brown	238	1:2	80	51.07	5.01	4.42	[Fe(C ₂₇ H ₃₀ O ₁₄) ₂ (H ₂ O) ₂] Cl
					50.49	4.99	4.35	
4	Blueish green	204	1:1	86	46.99	4.63	9.03	[Co(C ₂₇ H ₃₀ O ₁₄) H ₂ O Cl]
					46.93	3.88	8.54	
5	Dark green	222	1:1	84	45.89	5.00	8.37	[Ni(C ₂₇ H ₃₀ O ₁₄)(H ₂ O) ₂] Cl
					45.75	4.80	8.29	
6	White	218	1:1	90	46.55	4.80	9.44	[Zn(C ₂₇ H ₃₀ O ₁₄) H ₂ O Cl]
					46.49	4.59	9.38	

Infrared spectroscopic study

The characteristic vibrations of important groups are described in Table 2. The strong band at 1710 cm⁻¹ is attributed to (ν_{C=O}) group²⁰, was shifted to a lower frequency by 15-8 cm⁻¹ in the all the complexes as compared to its ligand (**L**). A broad band observed at 3700 cm⁻¹ in IR spectra of ligand (**L**) assigned to ν(OH), which was found to have disappeared in all the respective complexes (**1-6**) that means its bonding with metal ions through deprotonation^{20,21}. Another important ligand band occurring at 1275 cm⁻¹ due to phenolic ν(C-O) shifts to a lower frequency by 22-10 cm⁻¹ in the all complexes. Ligand behaved as bi dentate with one metal ion, through two-donor atoms of oxygen of carbonyl group and oxygen of the hydroxyl group. These observations were further indicated by the appearance of νM-O and νM-Cl, respectively²². All the complexes show additional bands at 840-830 cm⁻¹ indicating the presence of coordinated water^{22,23}.

Table 2: Stretching vibrational frequencies (cm⁻¹) located in the FT-IR spectra of L and its complexes

Comp. No.	$\nu_{C=O}$	ν_{OH}	ν_{C-O}	ν_{M-Cl}	ν_{M-O}	ρ_{O-H} of H ₂ O
(L)	1710	3700	1275	-	-	-
(1)	1702	-	1255	-	522	840
(2)	1700	-	1253	-	516	838
(3)	1695	-	1260	-	508	830
(4)	1699	-	1265	399	513	833
(5)	1700	-	1257	-	505	838
(6)	1697	-	1261	400	511	830

Electronic absorption spectra, magnetic susceptibility and conductivity measurement

The ligand (L) exhibited two high intensity bands in ethanol. The first bands appeared at 36359 and 38613 cm⁻¹, respectively and the second bands appeared at 32998 and 31655 cm⁻¹. The two first bands were attributed to $\pi \rightarrow \pi^*$ transitions of the carbonyl group and to conjugated ring system, respectively, while bands related to $n \rightarrow \pi^*$ transition may be masked by the extension of the second band²³.

Complexation of L with metal ions caused bathochromic shift with the appearance of new bands in the visible and near IR regions. These bands were attributed to M-L charge transfer and to ligand field transitions²⁴. Table 3 describes bands of maximum absorption of complexes (1-6) in dichloromethane with their assignments.

The spectra of Cr(III) complex (1) exhibited three absorption bands at 12364, 16493 and 29881 cm⁻¹. The spectrum was typical of octahedral Cr(III) complexes²⁵⁻²⁷. The (ν_2/ν_1) ratio is 1.33, which is very close to the value of obtained for pure octahedral Cr(III) complexes^{26,27}. Magnetic moment of solid complex was found to be 3.89 B.M. and conductivity in DMF showed that the complex was ionic (Table 3).

The UV-Vis spectrum of the yellowish brown manganese complex (2) shows two main absorption bands at 20294 and 29674 cm⁻¹, which indicate an octahedral geometry²⁵. The value of Racah parameters (10 Dq, B', β and ν_1) have been calculated to be 12238, 844, 0.98 and 11816 cm⁻¹, respectively. The effective magnetic moment at room temperature was found to be 5.02 B.M., which agree well for low-spin manganese in octahedral coordination²⁷. Conductivity measurement showed that the complex was not ionic (Table 3).

The prepared dark brown Fe(III) complex (3) showed three bands at 15018, 17803 and 33214 cm⁻¹, which are assigned to the transitions: ${}^6A_{1g} \rightarrow {}^4T_{1g}$, ${}^6A_{1g} \rightarrow {}^4T_{2g}$ and (L) \rightarrow Fe (C.T), respectively^{25,28,29}. The values of 10 Dq obtained by $Dq/B' = 1.2$, as well as B and β come out to 6818, 611 and 0.5, respectively^{25,28}. The magnetic moment of the present complex is 5.86 B.M., with five unpaired electrons and an octahedral configuration^{30,31}. The conductivity measurement in DMF showed that the complex was conducting, (Table 3); therefore (Cl) atoms was not considered to be coordinated with metal ion and is located outside the coordination zone.

The measured magnetic moment was 4.62 B.M. This show that the cobalt ion in it's bluish green complex to be paramagnetic with d⁷ configuration in a tetrahedral geometry^{27,30,31}. The electronic spectrum of cobalt complex (4) shows three bands at 14514, 16667 and 19802 cm⁻¹. These bands have been assigned to the transition ${}^4A_2 \rightarrow {}^4T_1(P)$ ²⁷⁻²⁹ assuming tetrahedral symmetry around Co(II) ion. The values of Racah

parameters (10 Dq, B', β and ν_2) have been calculated to be 3769.2, 698, 0.62 and 6310 cm^{-1} , respectively. The value of β (0.62) signifies a fair amount of covalent character in metal to nitrogen and oxygen bonds. While the value of 10 Dq to be 3769.2 cm^{-1} , one should expect a band due the transition ${}^4A_2 \rightarrow {}^4T_2(F)$ in the infrared region at (3749) cm^{-1} , which couldn't be observed in the spectrum of the cobalt (II) complex²⁷. Conductivity in DMF showed that the complex was not ionic (Table 3).

The electronic spectrum of nickel(II) complex (**5**) exhibited two main absorption bands, which are assigned to the two transitions ${}^1A_{1g} \rightarrow {}^1A_{2g}$ and ${}^1A_{1g} \rightarrow {}^1E_g$, respectively in the a square-planar geometry^{25,28,32}. Magnetic moment of the complex (0.08 B.M.) is higher than spin value of the nickel metal only, and this result indicates orbital contribution^{30,31}. Conductivity measurement showed that the complex was ionic (Table 3).

The complex (**6**) of zinc(II) is colorless and was diamagnetic as expected for d^{10} ion, since the UV-Vis spectra of the band position was compared with that of the ligand only. The conductivity measurements indicate a non-ionic behavior. Thus, from the data obtained from FT-IR spectrum and flame atomic absorption, a tetrahedral geometry a round Zn(II) ion^{24,29} has been assigned.

Table 3: Electronic spectra (CH_2Cl_2), magnetic moment (B.M.) and conductance in (DMF) for complexes (1-6)

No.	Maximum absorption ν_{max} (cm^{-1})	Band assignment	B'	β	10 Dq	Molar cond. $\text{S.cm}^2.\text{mol}^{-1}$	μ_{eff} B.M.	Suggested geometry
1	12364	${}^4A_{2g} \rightarrow {}^4T_{2g}$	-	-	-	70.94	3.89	O.h
	16493	${}^4A_{2g} \rightarrow {}^4T_{1g}$						
	29881	${}^4A_{2g} \rightarrow {}^4T_{1g}(P)$						
2	11816 (Cal.)	${}^6A_{1g} \rightarrow {}^4T_{1g}(G)$	844	0.98	12238	11.36	5.02	O.h
	20294	${}^6A_{1g}(S) \rightarrow {}^4T_{2g}(G)$						
	29674	${}^6A_{1g}(S) \rightarrow {}^4A_{1g} + {}^4E_g(G)$						
	36765	C.T						
3	15018	${}^6A_{1g} \rightarrow {}^4T_{1g}(G)$	611	0.5	6818	78.68	5.86	O.h
	17803	${}^6A_{1g}(S) \rightarrow {}^4T_{2g}(G)$						
	33214	C.T						
4	3749	${}^4A_2 \rightarrow {}^4A_2(F)$	698	0.62	3769.2	18.05	4.62	T.h
	6310 (Cal.)	${}^4A_2 \rightarrow {}^4T_2(F)$						
	16994	${}^4A_2 \rightarrow {}^4T_1(P)$						
5	16129	${}^1A_{1g} \rightarrow {}^1A_{2g}$	-	-	-	68.33	0.08	S.p
	23310	${}^1A_{1g} \rightarrow {}^1E_g$						
6	-	-	-	-	-	13.44	0.0	T.h

Stereochemistry of the structures of metal complexes (1-6)

According to the results obtained from elemental and spectral analysis as well as magnetic moment and conductivity measurements, the structure of the above mentioned compounds can be illustrated as follows (Fig. 2).

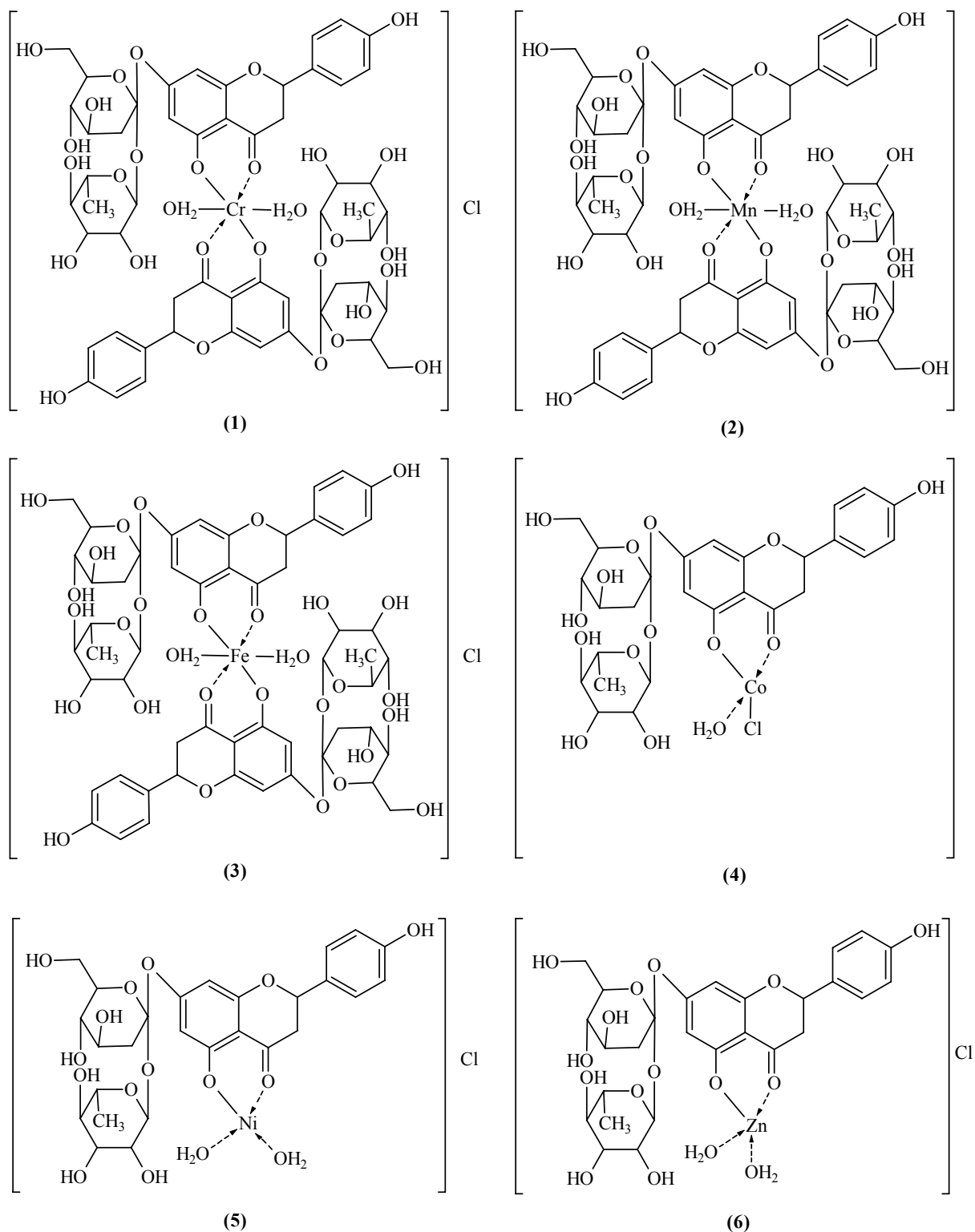


Fig. 2: The suggested structures of complexes (1-6)

Biological studies

The free ligand (L) and its complexes (1-6) were screened *in vitro* for their ability to inhibit the growth of representative bacteria *E. coli* as gram negative and *Staph. aureus* as gram positive. The results

are shown in Table 4. Also the study was made against *Aspergillusflaveus* and *Penicillum Spp.* fungi, in DMSO as a solvent (Table 4).

As a result from the above mentioned studies, the following points were concluded –

- (a) **(L)** was not active against *Staph.* and *E. coli*.
- (b) All complexes **(1-6)** showed high activity against two types of bacteria compared to the ligand **(L)** active prepared them.
- (c) Results of the antifungal activity of the new compounds showed that the metal ion chelates **(1-6)** were more toxic compared with their parent ligand **(L)** toward the same micro-organism and under the identical experimental conditions. The increase in the antifungal activity of metal chelates may be due to the effect of the metal ion on the normal cell process. These activities may be explained by Tweedy's chelation theory³³, according to which chelation reduces the polarity of the metal atom mainly, because of the partial sharing of its positive charge with the donor groups of the ligand, which favours permeation of the complexes through the lipid layer of cell membrane³⁴.

Table 4: Antibacterial and antifungal activities for ligand (L) and their metal complexes (1-6) (10^{-3} mgm.mL⁻¹)

Comp. No.	<i>E. coli</i>	<i>Staph. Aureus</i>	<i>Asp. Flavus</i>	<i>Penci. SPP.</i>
Control DMSO	-	-	-	-
(L)	-	-	44	36
(1)	8	6	22	30
(2)	6	10	17	19
(3)	6	-	28	30
(4)	6	6	28	30
(5)	-	6	26	20
(6)	10	6	18	15

Where: (+) 6-8, (++) 8-10, (+++)
(++++)
10>

Where: (+++) 30-40, (++++)
(+++++) 20-30, (+++++) 10-20

Study of complexes in gas state (Theoretical studies)

Electrostatic potentials

Electron distribution governs the electrostatic potential of the molecules. The electrostatic potential (E.P.) describes the interaction of energy of the molecular system with a positive point charge. E.P. is useful for finding sites of reaction in a molecule; positively charged species tend to attack a molecule, where the electrostatic potential is strongly negative (electrophonic attack)³⁵. The E.P. of the free ligand **(L)** was calculated and plotted as 2D contour to investigate the reactive sites of the molecules (Fig. 3). Also one can interpret the stereochemistry and rates of many reactions involving “soft” electrophiles and nucleophiles in terms of the properties of frontier orbital (HOMO, highest occupied molecular orbital) and (LUMO, lowest unoccupied molecular orbital). The results of calculations show that the LUMO of transition metal ions prefer to react with the HOMO of two-donor atoms of oxygen of carbonyl and oxygen of the hydroxyl group for Naringin free ligand **(L)**.

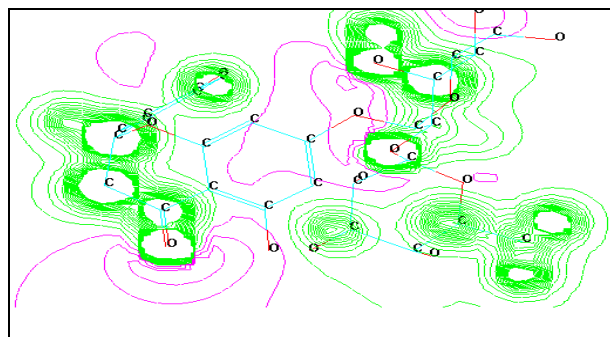


Fig. 3: Electrostatic potential (HOMO and LUMO) as 2D contours for (L)

Optimized energies

The program Hyperchem-8 was used for the semi-empirical and molecular mechanics calculations. The heat of formation (ΔH_f°) and binding energy (ΔE_b) for free ligand (**L**) and their metal complexes (**1-6**) were calculated (Table 5).

Table 5: Conformation energetic (in KJ. mol⁻¹) for Naringin and its metal complexes

Compd. No.	ΔE_{tot}	ΔH_f°	ΔE_b
L	-80673.95	35.07	-5200.37
1	-185054.96	-84.88	-10681.47
2	-113605.75	-266.77	-5662.60
3	-119290.09	-85.25	-5481.49
4	-122833.58	-98.94	-5607.85
5	-96003.98	-36.79	-5361.40
6	-137008.36	-15.17	-8153.68

The vibrational spectra of the free ligand (**L**) and their metal complexes (**1-6**) have been calculated, (Table 6). The theoretically calculated wave numbers for this ligand showed some deviations from the experimental values, and these deviations are generally acceptable in theoretical calculations³⁶. The most diagnostic calculated vibrational frequencies were chosen for the assignment of ligand (**L**) and metal complexes (**1-6**), and their respective experimental vibrational modes (Table 6).

Table 6: Comparison between the experimental and theoretical vibrational frequencies (cm⁻¹) for free ligand (L) and its metal complexes (1-6)

Compd. No.	$\nu_{C=O}$	ν_{C-O}	ν_{OH}	ν_{M-O}	ν_{M-Cl}	ρ_{O-H} of H ₂ O
L	1715*	1270*	3706*	-	-	-
	1710**	1275**	3700**			
(1)	1699*	1260*	-	545*	-	844*
	1700**	1255**		522**		840**

Cont...

Compd. No.	$\nu_{C=O}$	ν_{C-O}	ν_{OH}	ν_{M-O}	ν_{M-Cl}	ρ_{O-H} of H_2O
(2)	1699*	1250*	-	515*	-	840*
	1700**	1253**		516**		838**
(3)	1700*	1258*	-	505*	-	844*
	1695**	1260**		508**		830**
(4)	1705*	1260*	-	512*	379*	828*
	1699**	1265**		513**	399**	833**
(5)	1665*	1255*	-	554*	-	829*
	1700**	1257**		505**		838**
(6)	1700*	1259*	-	554*	395*	828*
	1697**	1261**		511**	400**	830**

Where *Theoretical frequency, **Experimental frequency

The results obtained for the theoretical calculations of the frequencies agreed well with those obtained for the experimental values (Tables 2).

Bond length measurements for the (L) and its metal complexes (1-6)

Calculation of parameters has been optimized for bond lengths of the free ligand (L) and their metal complexes by applying the semi-empirical (PM3) at geometry optimization (0.001 K.Cal.mol⁻¹), which gives excellent agreement with the experimental data^{37,38} (Table 7).

Table 7: Selected bond lengths (Å) for ligand and its metal complexes¹⁻⁶

Compd. No.	C=O	C-O	M-O	M-Cl
L	1.62	1.50	-	-
(1)	1.67	1.55	2.28	-
(2)	1.71	1.58	2.25	-
(3)	1.69	1.55	2.22	-
(4)	1.65	1.53	2.28	1.92
(5)	1.70	1.56	2.14	-
(6)	1.63	1.54	2.19	1.89

Theoretical electronic spectra for the metal complexes (1-5)

The electronic spectra of the metal complexes have been calculated and the wave number for these compounds showed some deviations from the experimental values as shown in Table 8. These deviations in theoretical calculation are generally acceptable due to couplings between the electronic spectra modes and the approximation that each normal mode of the electronic spectra interacts independently electronic spectra beam^{39,40}. The most diagnostic calculated electronic spectra were chosen for the assignment of the metal complexes¹⁻⁵. Experimental electronic modes are shown in Table 3. The theoretical electronic spectra of all compounds were calculated by using the semi-empirical (PM3) method at geometry optimization (0.01 K.Cal. Mol⁻¹), and the comparison was made between the experimental data and theoretical data of the electronic spectra for¹⁻⁵ metal complexes (Table 8).

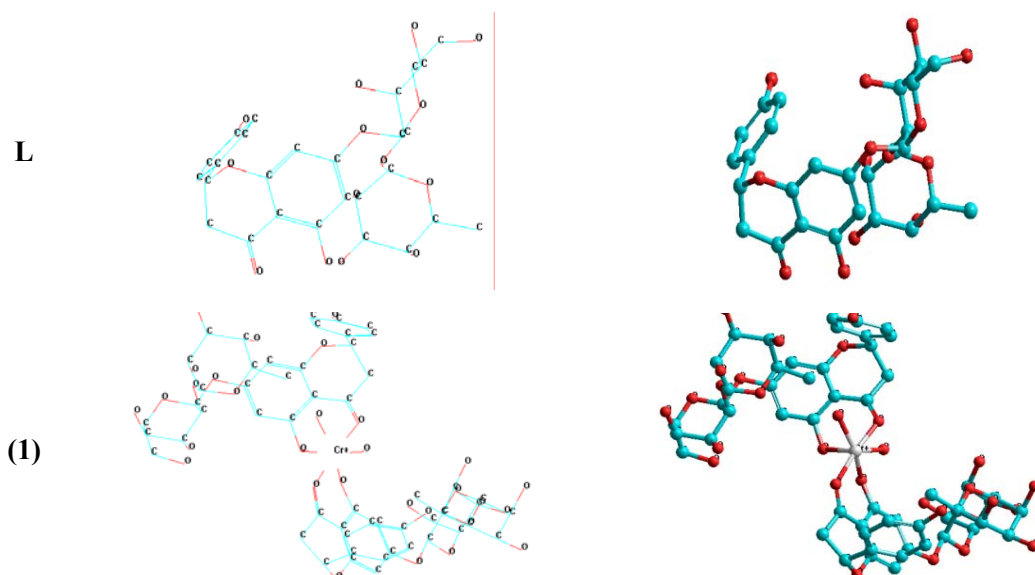
Table 8: Comparison between experimental and theoretical of the electronic spectra for (1-5) complexes

Symb.	Maximum absorption $\nu_{\max}(\text{nm})$	Band assignment	Suggested geometry
(1)	810*, 808**	${}^4A_{2g} \rightarrow {}^4T_{2g}$	O.h
	628*, 606**	${}^4A_{2g} \rightarrow {}^4T_{1g}$	
	350*, 334**	${}^4A_{2g} \rightarrow {}^4T_{1g}(\text{P})$	
(2)	866*, 846**	${}^6A_{1g} \rightarrow {}^4T_{1g}(\text{G})$	O.h
	498*, 492**	${}^6A_{1g}(\text{S}) \rightarrow {}^4T_{2g}(\text{G})$	
	340*, 336**	${}^6A_{1g}(\text{S}) \rightarrow {}^4A_{1g} + {}^4E_g(\text{G})$	
	290*, 271**	C.T	
(3)	688*, 665**	${}^6A_{1g} \rightarrow {}^4T_{1g}(\text{G})$	O.h
	548*, 561**	${}^6A_{1g}(\text{S}) \rightarrow {}^4T_{2g}(\text{G})$	
	311*, 301**	C.T	
(4)	2682*, 2667**	${}^4A_2 \rightarrow {}^4A_2(\text{F})$	T.h
	1590*, 1584**	${}^4A_2 \rightarrow {}^4T_2(\text{F})$	
	592*, 588**	${}^4A_2 \rightarrow {}^4T_1(\text{P})$	
(5)	630*, 620**	${}^1A_{1g} \rightarrow {}^1A_{2g}$	S.p
	443*, 429**	${}^1A_{1g} \rightarrow {}^1E_g$	

Where *Theoretical frequency, **Experimental frequency

Optimized geometries of (L) and their complexes (1-6)

All theoretically probable structures of free ligand (**L**) and its complexes have been calculated by (PM3) method in gas phase to search for the most probable model building stable structure (Fig. 4).



Cont...

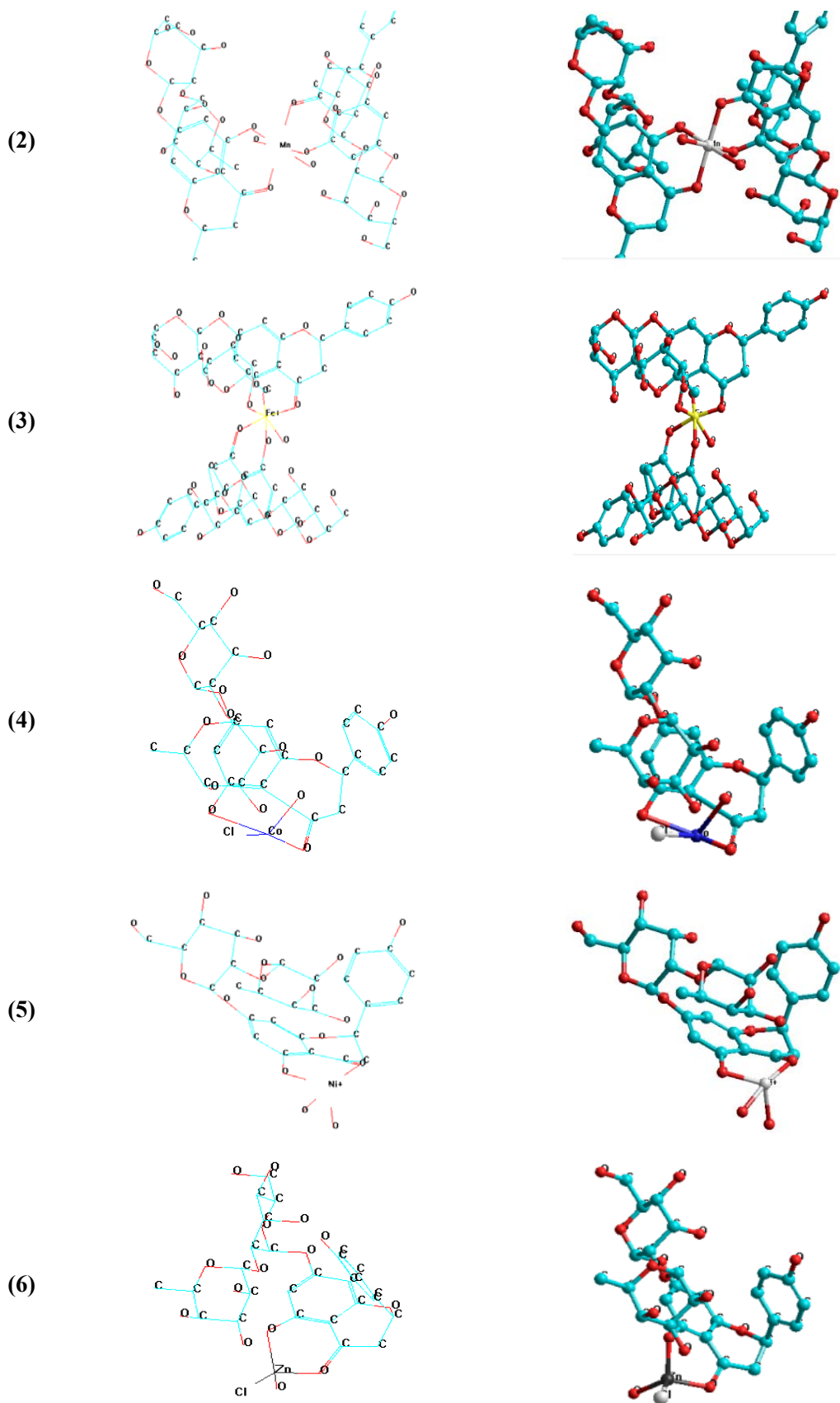


Fig. 4: Conformational structure of (L) and its metal complexes (1-6)

REFERENCES

1. W. L. Bear and R. W. Teel, Effect of Citrusphytochemicals on Liver and Lung Cytochrome P450 Activity and on the *In Vitro* Metabolism of the Tobacco Specific Nitrosamine NKP, *Anticancer Res.*, **20**, 3323-3329 (2000).
2. Y. Yamamoto and R. B. Gaynor, Therapeutic Potential of Inhibition of the NF- κ B Pathway in the Treatment of Inflammation and Cancer, *J. Clin. Invest.*, **107**, 135-142 (2001).
3. G. G. Duthic, S. J. Duthic and J. A. M. Kyle, Plantpolyphenols in Cancer and Heart Disease: Implications Asnutritional Antioxidants, *Nutr. Res. Rev.*, **13**, 79-106 (2000).
4. T. P. T. Cushnie and A. J. Lamb, Antimicrobial Activity of Flavanoids, *Int. J. Antimicrob. Agents*, **26**, 343-356 (2005).
5. J. P. E. Spencer, Flavonoids: Modulators of Brain Function, *Brit. J. Nutr.*, **99**, ES60-ES77 (2008).
6. S. V. Jovanovic, S. Steenken, M. Tosic, B. Marjanovic and M. G. Simic, Flavonoids as Antioxidants, *J. Am. Chem. Soc.*, **116**, 4846-4851 (1994).
7. G. C. Jagetia, V. A. Venkatesha and T. K. Reddy, Naringin, A Citrus Flavonone, Protects against Radiation Induced Chromosome Damage in Mouse Bone Marrow, *Mutagenesis*, **18**, 337-343 (2003).
8. R. Schindler and R. Mentlein, Flavonoids and Vitamin E Reduce the Release of the Angiogenic Peptide Vascular Endothelial Growth Factor from Human Tumor Cells, *J. Nutr.*, **136**, 1477-1482 (2006).
9. M. J. Martin, E. Marhuenda, C. Perez-Guerrero and J. M. Franco, Antiulcer Effect of Naringin on Gastric lesions Induced by Ethanol in Rats, *Pharmacol.*, **49**, 144-150 (1994).
10. P. B. Gordon, I. Holen and P. O. Seglen, Protection, Bynaringin and Some other Flavonoids, of Hepatocyticautophagy and Endocytosis against Inhibition by Okadaic Acid, *J. Biol. Chem.*, **270**, 5830-5838 (1995).
11. Y. F. Ueng, Y. L. Chang, Y. Oda, S. S. Park, J. F. Liao, M. F. Lin and C. F. Chen, *In Vitro* and *In Vivo* Effects of Naringin on Cytochrome p-450-depenent Mono Oxygenase in Mouse Liver, *Life Sciences*, **65**, 2591-2602 (1999).
12. S. Kanno, A. Shouji, K. Asou and M. Ishikawa, Effect of Naringin on Hydrogen Peroxide-induced Cytotoxicity and Apoptosis in P 388 Cells, *J. Pharmacol. Sci.*, **92**, 166-170 (2003).
13. H. Zhang, C. W. Wong, P. F. Coville and S. Wanwimolruk, Effect of the Grapefruit Flavonoid Naringin Onpharmacokinetics of Quinine in Rats, *Drug Metabol. Drug Interact.*, **17**, 351-363 (2000).
14. D. Skoog, *Fundamental Analytical Chemistry*, New York (1988).
15. J. J. Stewart, *Reviews in Computational Chemistry*, K. B. Lipkowitz, D. B. Boyd (Eds.), VCH Publishers, New York, **(1)9**, 72-80 (1996).
16. D. B. Cook, *Hand Book of Computational Quantum Chemistry*, New York, Oxford Univ. Press, 149 (1998).
17. H. Choinacki and F. Pruchnik, Quantum Chemical Studies on Molecular and Electronic Structure of Complexes Adducts, *Int. J. Mol. Sci.*, **2(44)**, 11-17 (2001).
18. T. T. Nahari, Synthesis, Ab initio and PM3 Studies of the 2-(5-mercapto-4H-1,2,4-triazol-3-yl)phenol and some of their Transition Metal Complexses, *Isesco Sci. Technol. Vision*, **3(3)**, 32-40 (2007).

19. M. R. Atlas, E. Alfres and C. L. Parks, Laboratory Manual Experimental Microbiology, Mosby – Year Book, Inc. (1995).
20. V. M. Parikh, Absorption Spectroscopy of Organic Molecules, John-Wiley and Sons (1974).
21. D. Dolphin and A. Wick, Tabulation of Infrared Spectral Data, John Wiley and Sons, New York (1977).
22. K. Nakamoto, Infrared Spectro of Inorganic and Coordination Compounds, 6th Ed., Wiley, Inter Science, New York (1997).
23. R. M. Silverstein, G. C. Bassler and T. C. Morrill, Spectrometric Identification of Organic Compounds, 4th Ed., John Wiley and Sons Inc., New York (1981).
24. J. C. Bailar, H. Emeleus and R. Nyholm, Comprehensive Inorganic Chemistry, Pergamon Press (1973).
25. B. N. Figgis, Introduction to Ligand Field, Interscience, New York (1966).
26. D. Sutton, Electronic Spectra of Transition Metal Complexes, McGraw – Hill, Publishing, London (1968).
27. N. N. Greenwood and A. Earnshaw, Chemistry of Elements, 2nd Ed., Prigaman Press (1998).
28. C. Ballhausen, Introduction to Ligand Field Theory, New York, Toronto – London (1962).
29. D. Nicholis, Complexes and First-Row Transition Elements, Translated by W. I. Azeez (1984).
30. R. L. Carlin and A. J. Van Duyneveldt, Magnetic Properties of Transition Metal Compounds, New York (1977).
31. R. L. Dutta and A. Shyamal, Element of Magnetochemistry, Affiliated East-West Press, New Delhi (1982).
32. A. B. P. Lever, Inorganic Electronic Spectroscopy, Elsevier Amsterdam (1968).
33. C. H. Collins and P. M. Lyne, Microbiological Methods, Butter Worth Co. Ltd., 3rd Ed. (1970).
34. J. E. Huheey, Inorganic Chemistry, Principles of Structure and Reactivity, Harper International Edition Harper and Row, Publishers, New York, 1st Ed (1972).
35. K. Nagesha and A. Kotove, Concepts in Theoretical Chemistry Elsevier Publishing Company, New York, London (1978).
36. A. A. Azhary, J. Phys. Chem., **102**, 620-629 (1998).
37. D. Kunkeler, J. Cornelissen and K. Ree Dig, J. Am. Chem. Soc., **118**, 2190-2197 (1996).
38. H. Keypour, K. P. Wainwright and M. Taylor, J. Iran. Chem. Soc., **1(1)**, 53-64 (2004).
39. C. Henryk, K. Wojciech and P. Florian, Quantum Chemical Studied on Molecular and Electronic Structure of some Metal Complexes, Int. Mol. Sci., **2** (2001).
40. D. K. Nagesha and N. A. Kotov, Electronic Structure of CDS Nanoparticles Modified at the Chalcogen Sites and Luminescence Effects, Material, **8(4)** (2003).